Electronic Supplementary Material (ESI) for Soft Matter

Electronic Supplementary Information

2D Dendritic Fractal Patterns from an Amphiphilic Polysaccharide

*Elina Niinivaara, Eero Kontturi**

Table of Contents

1. Total surface free energy

The Fowke's method works in such a way that it divides the total surface free energy into two components; the dispersive component (Υ^d) and the polar component (Υ^p). Using a geometric mean approach, the contributions of both components are combined. When combined with Young's equation the Fowke's equation becomes

$$\gamma_l(1 + \cos\theta) = 2\left(\sqrt{\gamma_l^p \gamma_s^p} + \sqrt{\gamma_l^d \gamma_s^d}\right) \tag{1}$$

Where θ is the contact angle and γ is the surface tension for the liquid, l, and solid, s. Simplified, the total surface free energy is then

$$\gamma_s = \gamma_s^p + \gamma_s^d \tag{2}$$

The Fowke's method as a tool for calculating the surface free energy has been heavily criticized.[S1] However, we believe that it is a sound method for observing the relative differences between the surface energies of the substrates.

Table S1. Surface tension values for probe liquids. Surface tension values are further divided into their components; Υ^{d} the dispersive component and the Lewis acid (Υ^{+}) and Lewis base (Υ^{-}) components of the polar component, Υ^{p} [S2]

Probe Liquid	Υ	Υ^{d}	Υ^{+}	Υ^{-}
Water	72.80	21.80	25.50	25.50
Diiodomethane	50.80	50.80	0.00	0.00
Formamide	58.00	39.00	2.28	38.10
Ethylene Glycol	48.00	29.00	1.92	47.00

Table S2. Equilibrium contact angles (at 3 min) of all four probe liquids for a) hydrophilic silica, b) mica, c) HOPG and d) hydrophobic silica.

a)

Probe Liquid	θ
Water	0.00
Diiodomethane	34.78
Formamide	0.00
Ethylene Glycol	0.00

b)

Probe Liquid	θ
Water	0.00
Diiodomethane	39.48
Formamide	0.00
Ethylene Glycol	19.22

c)

Probe Liquid	θ
Water	87.94
Diiodomethane	8.99
Formamide	66.80
Ethylene Glycol	60.44

d)

Probe Liquid	θ
Water	94.47
Diiodomethane	70.46
Formamide	93.78
Ethylene Glycol	85.85

3. Substrate dependent monolayer morphology

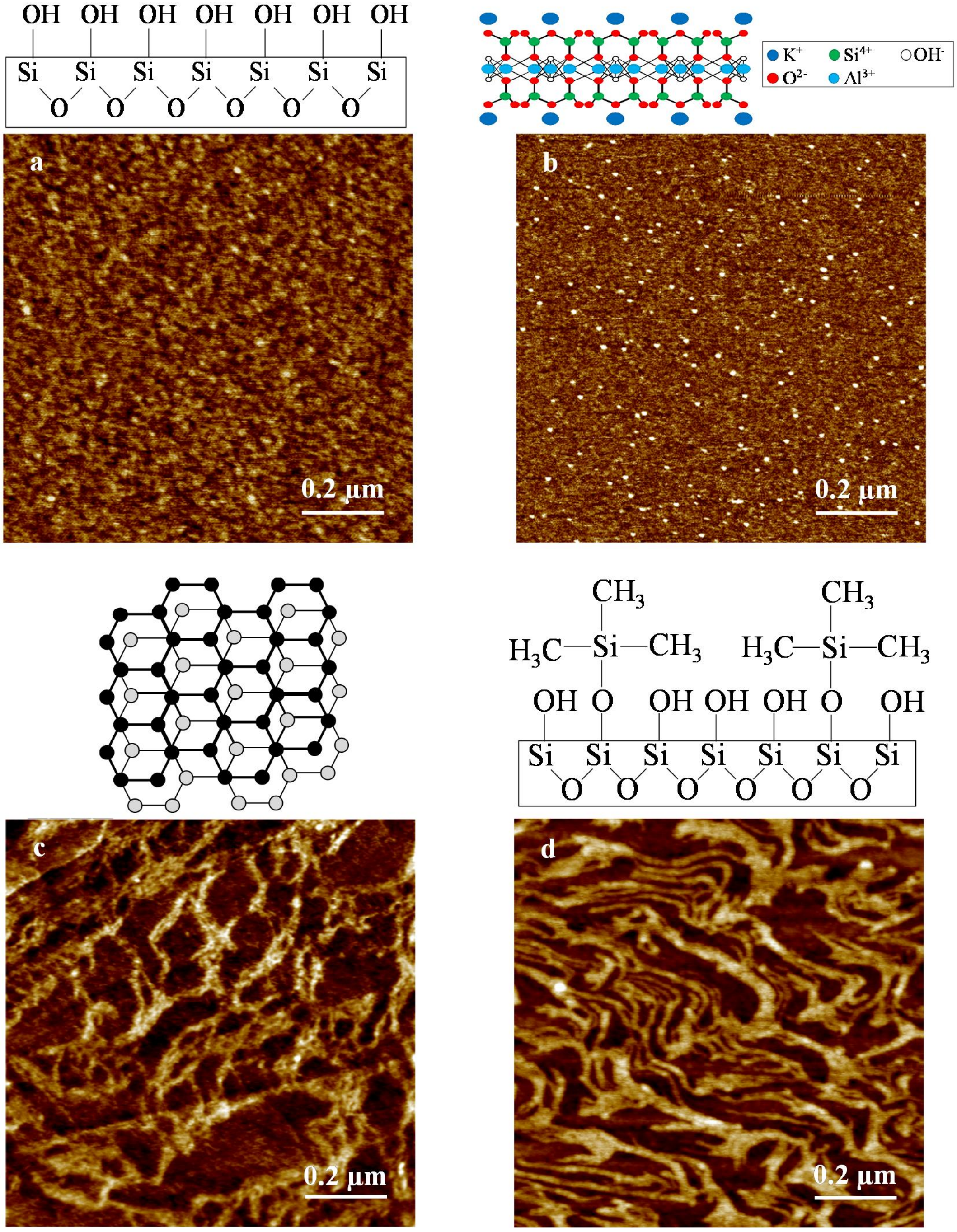

Fig. S1. 1×1 µm^2 AFM images of a TMSC monolayer on a) hydrophilic silica b) mica c) HOPG and d) hydrophobic silica.

4. X-ray diffraction

Grazing incidence x-ray diffraction (GIXRD) measurements from thin films were conducted at the Beamline W1.1 at the Hamburger Synchrotronstrahlungslabor of the Deutsches Electronen Synchrotron (DESY). The beam was monochromatized with a double crystal Si(111) monochromator, and X-ray energy 10.5 keV was used. The beam was narrowed with slits to 0.2 × 1 mm, and the diffraction pattern was recorded with a flat image plate at 297 mm distance. The angle of incidence was ω = 0.12°.

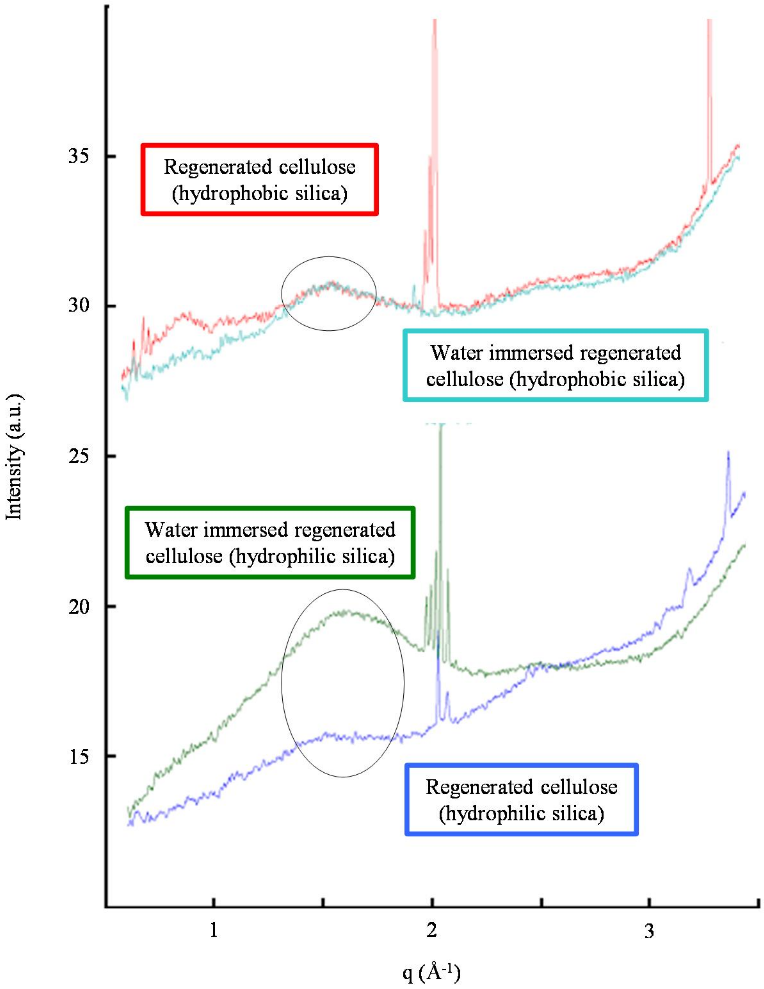

Fig. S2. X-ray diffraction pattern of cellulose on hydrophilic silica (blue), cellulose on hydrophilic silica immersed in water for 15 min and subsequently dried for 48 h (green), cellulose on hydrophobic silica (red) and cellulose on hydrophobic silica immersed in water for 15 min and subsequently dried for 48 h (turquoise).

The results shown in the x-ray diffraction patterns above indicated that no long range order could be detected in the TMSC or regenerated cellulose films on the hydrophobized silica substrate. The diffraction patters of all four samples measured all resemble one another and so give no evidence for a change in crystallinity upon factal formation on the hydrophobic silica.

5. Time independent fractal formation

Time independency was examined by altering the time of deposition during film formation. The substrate was brought into contact with the TMSC monolayer on the water subphase and film formation was allowed to take place for 10, 30 and 120 seconds before the substrate was retracted from the monolayer into the air.

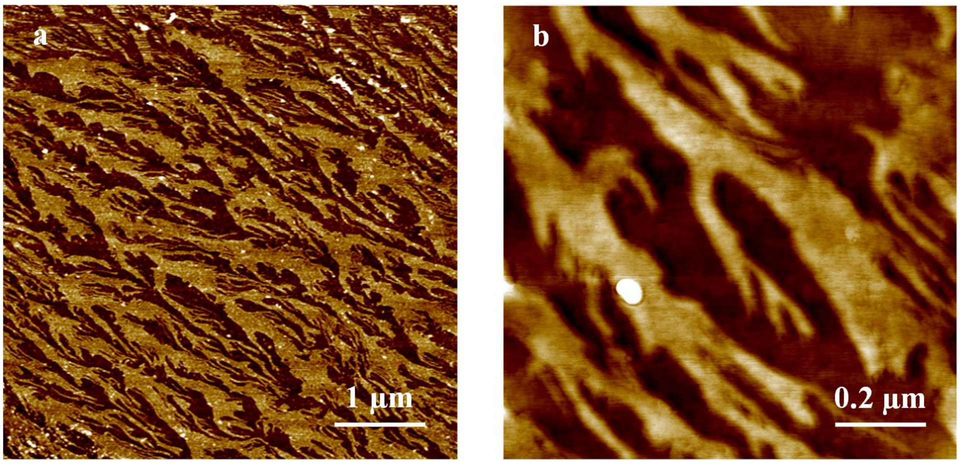

Fig. S3. a) 5×5 µm^2 and b) 1×1 µm^2 AFM images of a TMSC monolayer on hydrophobic silica deposited for 10 Seconds.

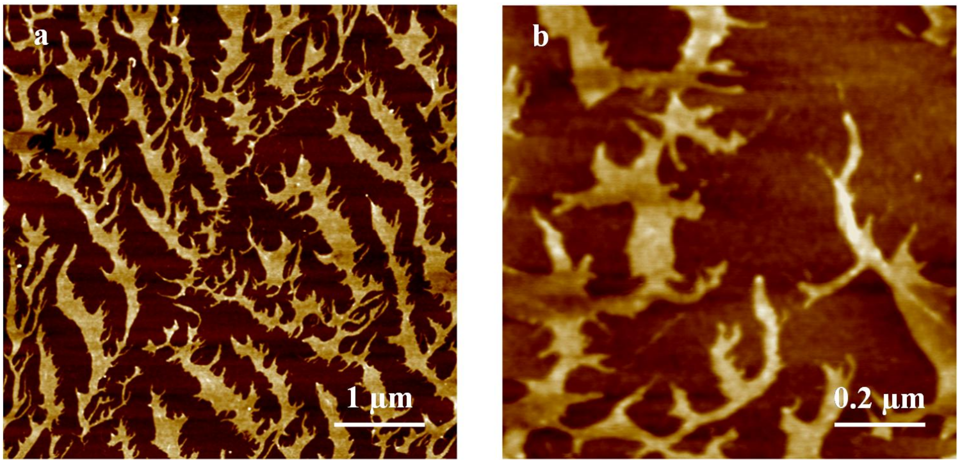

Fig. S4. a) 5×5 µm^2 and b) 1×1 µm^2 AFM images of a TMSC monolayer on hydrophobic silica deposited for 120 Seconds.

6. Fractal dimensions

Fractal dimensions were calculated using the box counting method. Calculations were carried out using fractal box count analysis tool of the ImageJ 1.44p software. AFM images were first converted to black and white and thresholded using Adobe Photoshop CS6 after which they were made into binary images consisting of only the outline of the fractals using ImageJ. The binary images were then used in the fractal dimension calculations.

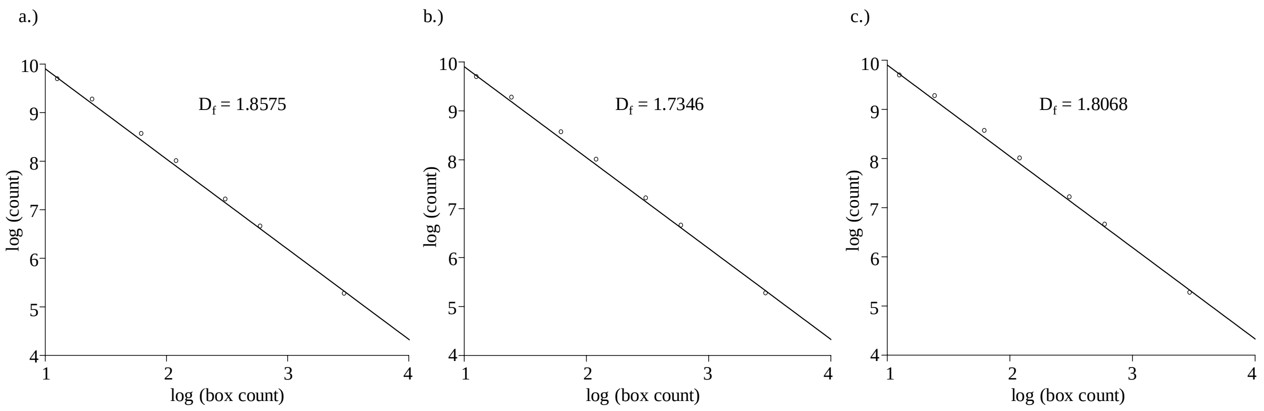

Fig. S5. Log-log plot of boxcount results for the on a.) TMSC fractals b.) regenerated cellulose fractals and c.) regenerated cellulose immersed in water fractals on hydrophobic silica. The slope of the line indicates the fractal dimension of the 2 dimensional film.

7. Hydrolysis of TMSC

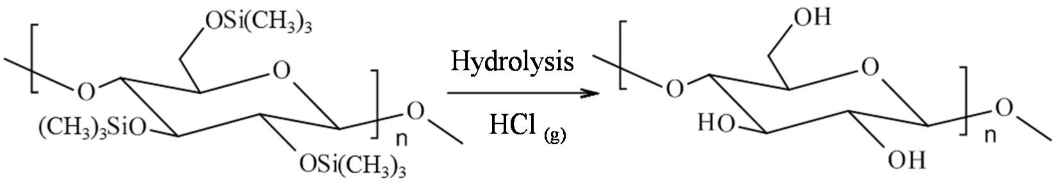

Fig. S6. The regeneration of trimethylsilyl cellulose to cellulose occurs through a hydrolysis mechanism in the presence of hydrochloric acid vapor.

8. TMSC fractal pattern height profile

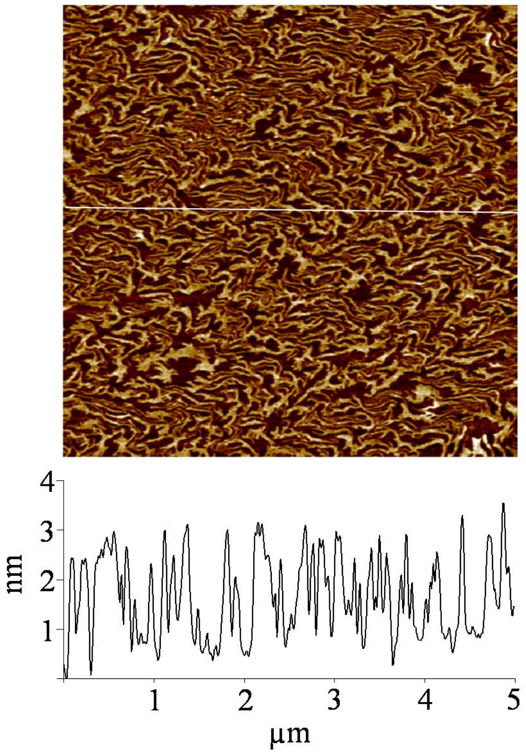

Fig. S7. 5×5 μm^2 AFM image of TMSC monolayer on hydrophobic silica including height profile. The white line indicates the place on the image from where the height profile as been measured.

9. Volumetric analysis of material in AFM images

The material volume of the polymer layer on the hydrophobic substrate was quantified from the AFM images using Scanning Probe Image Processor (SPIP) 6.0.6 software. Using the particle and pore analyzer tool, the AFM images were thresholded and the material volume and coverage of the polymer, indicated by the thresholding, were calculated by the software. 5×5 µm^2 Thresholded AFM images for TMSC, regenerated cellulose and cellulose immersed in water can be seen in Figure S8.

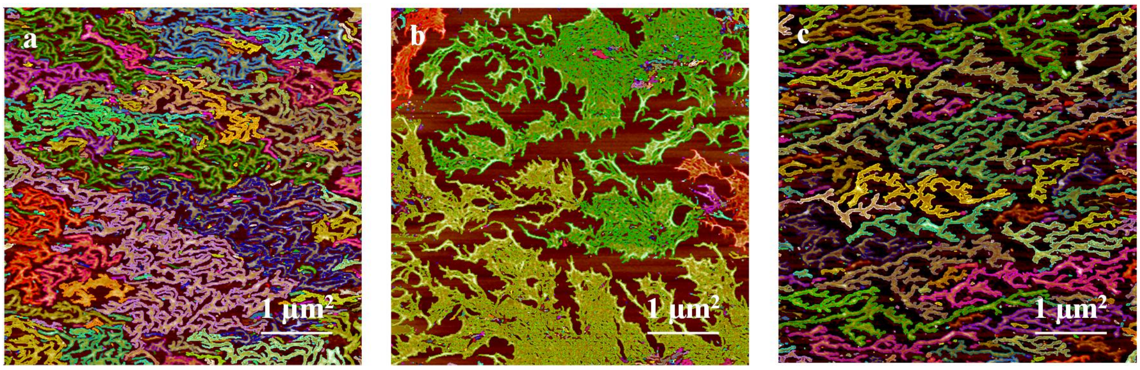

Fig. S8. Thresholded AFM images of a) TMSC b) regenerated cellulose and c) cellulose immersed in water on hydrophobic silica. The colors in the images indicate groups of particles of similar size detected by the image analysis software. Particles of the same size are assigned the same, unique color.

Material volumes for the three samples are shown in Table S3. The volumes presented here cannot be considered absolute values due to the fact that both the thresholding and the scratching technique are always subject to interpretation. Although material is stoichiometrically lost upon the hydrolysis of TMSC to cellulose (Figure S6), the apparent increase in the volume of cellulose in contrast to TMSC is probably due to the water uptake of hygroscopic cellulose. Therefore, the values between TMSC and cellulose are not directly comparable, but it is highly implausible the reaction between HCl vapor and TMSC could reduce or increase the number of actual polymer chains in the film. The comparable and similar values between two cellulose samples, on the other hand, strongly suggest that there is no loss of material upon water immersion of cellulose, merely molecular rearrangements.

Table S3. The coverage, material volume in nm^3 and $\times 10^{-14}$ cm^3 of TMSC, regenerated cellulose and cellulose immersed in water on hydrophobic silica. Coverage and material volume were measured for a surface area of 5×5 μm^2.

	Coverage %	Material volume nm^3	Material Volume cm^3 ($\times 10^{-14}$)
TMSC on hydrophobic silica	42.65	18308081	1.83
Cellulose on hydrophobic silica	41.10	28951617	2.90
Cellulose after immersion in water on hydrophobic silica	34.52	28161165	2.82

10. Hydrophobized silica substrates

The hydrophobized silica substrates were prepared by methylation of the native oxide layer in cleaned pristine (hydrophilic) silicon substrates (see Experimental section). The chemical composition of the substrates was analyzed using XPS (Table S4). The XPS results show that on average 93.5% of the surface carbon is bound to silicon in the form of a C-Si bond indicating almost full coverage and successful methylation of the pristine silica substrate.

X-ray photoelectron spectroscopy (XPS) was utilized to ascertain the uniformity of methyl group on the hydrophobized silica surface by comparing its XPS spectrum to that of hydrophilic silica. The XPS data was collected using a Kratos AXIS Ultra electron spectrometer with an alumiunium anode (mono Al Kα) operated at 100W. Positive charges caused by photoelectric emission were neutralized. Samples were pre-evacuated overnight. For the hydrophobized silica, two spots on two samples were measured and for the hydrophilic silica, three spots on two samples. Data was collected from an area of ~1 mm in diameter as an electron take-off angle of 90°. Low-resolution measurements (160 eV and 1 eV step) were used to analyze elemental compositions whereas high-resolution measurements (20 eV and 0.1 eV step) were used to analyze surface chemistry. The spectra from the hydrophobized and hydrophilic substrates were compared by correcting the hydrophobized substrate spectra with the Si 2p position from the hydrophilic substrate spectra. This was carried out to determine the binding energy of Si-C on the hydrophobized silica.

Table S4. XPS data from the analysis of the hydrophobized silica. Atomic concentrations are from wide scan data and the C1s high resolution components have been achieved with deconvolution of C1s emission.[S3]

	Atomic Concentrations, wides (AC's)			C 1s HiRes components				
	O 1s, %	C 1s, %	Si 2p, %	C-Si, % 284.6 eV	C-C, % 285.0 eV	C-O, % 286.7 eV	C=O, % 288 eV	COO, % 289 eV
Hydrophobized Silica, sample 1	33.1	15.7	51.3	90.1		5.6	2.6	1.8
	32.5	16.6	50.9	95.0		4.5	0.5	0.0
Hydrophobized Silica, Sample 2	34.1	16.2	49.6	93.1		4.8	1.7	0.5
	33.7	16.2	50.2	95.7		3.7	0.6	0.0
Pristine silica, sample 1	38.1	9.6	52.3		57.9	19.6	10.3	12.3
	37.2	8.1	54.7		58.2	18.4	9.4	14.0
	38.7	7.5	53.8		59.9	19.3	8.0	12.8
Pristine silica, sample 2	37.1	7.6	55.3		59.8	18.4 %	9.0	12.9
	37.4	7.2	55.5		60.3	20.0 %	9.1	10.7
	37.5	7.1	55.4		61.1	18.9 %	7.9	12.1

References

S1 E. Chibowski and R. Perea-Carpio, *Adv. Colloid Interface Sci.*, 2002, **98**, 245.

S2 C. Della Volpe and S.J. Siboni, *Adhesion Sci. Technol.*, 2000, **14**, 235.

S3 G. Beamson and D. Briggs *High resolution XPS of Organic Polymers*, Wiley, Chichester, 1992.